BAW-10255(NP)
Revision 2

Cycle-Specific DIVOM Methodology Using the RAMONA5-FA Code

January 2006

Framatome ANP, Inc.

ISSUED IN FRA-ANP ON-LINE
DOCUMENT SYSTEM
DATE: 1/30/06

BAW-10255(NP)
Revision 2

Cycle-Specific DIVOM Methodology Using the RAMONA5-FA Code

Prepared:	Y. Farawila Y. M. Farawila, Consultant	27.01.2006 Date
Prepared:	D. R. Tinkler, Engineer BWR Safety Analysis	1/30/06 Date
Reviewed:	Donald R Todd D. R. Todd, Engineer Systems Analysis Methods	30-Jan-06 Date
Reviewed:	D. N. Ziabletsev, Engineer Nuclear Technology	1/30/06 Date
Approved:	J. S. Holm, Manager Product Licensing	1/30/06 Date
Approved:	D. W. Pruitt, Manager Codes and Methods	1/28/06 Date

skm

U.S. Nuclear Regulatory Commission
Report Disclaimer

Important Notice Regarding the Contents and Use of This Document

Please Read Carefully

This technical report was derived through research and development programs sponsored by Framatome ANP, Inc. It is being submitted by Framatome ANP, Inc. to the U.S. Nuclear Regulatory Commission as part of a technical contribution to facilitate safety analyses by licensees of the U.S. Nuclear Regulatory Commission which utilize Framatome ANP, Inc. fabricated reload fuel or technical services provided by Framatome ANP, Inc. for light water power reactors and it is true and correct to the best of Framatome ANP, Inc.'s knowledge, information, and belief. The information contained herein may be used by the U.S. Nuclear Regulatory Commission in its review of this report and, under the terms of the respective agreements, by licensees or applicants before the U.S. Nuclear Regulatory Commission which are customers of Framatome ANP, Inc. in their demonstration of compliance with the U.S. Nuclear Regulatory Commission's regulations.

Framatome ANP, Inc.'s warranties and representations concerning the subject matter of this document are those set forth in the agreement between Framatome ANP, Inc. and the Customer pursuant to which this document is issued. Accordingly, except as otherwise expressly provided in such agreement, neither Framatome ANP, Inc. nor any person acting on its behalf:

a. makes any warranty, or representation, express or implied, with respect to the accuracy, completeness, or usefulness of the information contained in this document, or that the use of any information, apparatus, method, or process disclosed in this document will not infringe privately owned rights;

or

b. assumes any liabilities with respect to the use of, or for damages resulting from the use of, any information, apparatus, method, or process disclosed in this document.

Nature of Changes

Item	Page	Description and Justification
1.	Section 4.3 (page 4-4)	Updated UO2 to UO_2 for consistency.
2.	Section 4.6	Modified wording.
3.	Section 4.6.4	Added additional clarification on CPR correlations.
4.	Section 5.0 (page 5-1)	Added text for additional benchmarks.
5.	Section 5.1 (page 5-1)	Modified discussion to be consistent with current results.
6.	Section 5.2 (page 5-2)	Modified discussion to be consistent with current results.
7.	Section 5.3 (page 5-2)	Added new Section 5.3.
8.	Section 5.4 (page 5-2)	Added new Section 5.4.
9.	Section 5.5	Modified figures to be consistent with current results.
10.	Section 6.0 (page 6-1)	Added new sensitivity studies.
11.	Section 6.21 (page 6-7)	Modified discussion for sensitivity study.
12.	Section 6.24	Added new sensitivity study.
13.	Section 6.25	Added new sensitivity study.
14.	Section 6.26	Added new sensitivity study.
15.	Section 6.27	Added new sensitivity study.
16.	Table 6-1	Added new sensitivity studies.
17.	Figure 6-22	Updated results for sensitivity study.
18.	Figures 6-25, 6-26, 6-27, and 6-28	Added results of new sensitivity studies.
19.	Section 8.0 (page 8-2)	Updated format of References 19 and 20. Added Reference 21.

Contents

Tables

Figures

This document contains a total of 117 pages.

Nomenclature

BOC	Beginning of Cycle
BSP	Backup Stability Protection
BWR	Boiling Water Reactor
BWROG	BWR Owners' Group
CHF	Critical Heat Flux
CHFR	Critical Heat Flux Ratio
CHFRMIN	Critical Heat Flux Ratio Minimum
CPR	Critical Power Ratio
CSD	Cycle Specific DIVOM
D&S	Detect and Suppress
DIVOM	Delta CPR over Initial CPR Versus Oscillation Magnitude
EOFP	End of Full Power
FANP	Framatome ANP
FOM	Figure of Merit
GE	General Electric Company
HCOM	Hot Channel Oscillation Magnitude
ICA	Interim Corrective Action
LPRM	Local Power Range Monitor
MCPR	Minimum Critical Power Ratio
OPRM	Oscillation Power Range Monitor
PBDA	Period Based Detection Algorithm
PHE	Peak Hot Excess Reactivity
PWR	Pressurized Water Reactor
SLMCPR	Safety Limit MCPR
TM	Thermal Margin
TMMIN	Thermal Margin Minimum
USNRC	United States Nuclear Regulatory Commission

Abstract

The methodology for generating DIVOM curves based on cycle-specific analysis with the BWR transient system code RAMONA5-FA is presented in this report. The DIVOM curve is a relationship between the hot bundle relative oscillation magnitude and the limiting fractional change in critical power ratio. This report addresses the capabilities of the selected transient system code, RAMONA5-FA, the characteristics of the transient -- neutron-coupled density wave oscillations of the regional mode type -- and the range of input data defining the state points within the reload cycle for which the DIVOM curve is generated. It also addresses the procedure for post-processing the system code output to generate the DIVOM data consistent with their intended application as part of the long term stability solution Option III known as Detect & Suppress.

1.0 Introduction

This report describes the Framatome ANP, Inc.* (FANP) methodology for the evaluation of the critical power response of the core to regional oscillations on a cycle-specific basis. This response is characterized by the DIVOM curve. As the cycle-specific DIVOM methodology is part of a comprehensive long term stability solution which has been evolving for many years, Section 2 of this report is devoted to placing the present effort in a historical perspective. Section 3 is devoted to a detailed qualitative discussion of the physical phenomena pertinent to the DIVOM evaluation. With this background, the development campaign to prepare the transient system code, RAMONA5-FA, for the task of calculating DIVOM transients is put in perspective. The RAMONA5-FA code update is presented in Section 4. The validation of the code capabilities with regard to reactor oscillations as well as transient hydraulic test loop measurements is presented in Section 5. Having demonstrated the capability of the code to calculate a DIVOM transient, Section 6 presents the DIVOM sensitivity to input data variations to demonstrate that the methodology is robust. The remaining element of the methodology is the procedure specifying the set of transients starting at representative state points throughout the cycle, the criteria to select the limiting one, and the algorithm for extracting the DIVOM data from the transient output. This is described in the DIVOM procedure, Section 7.

* Framatome ANP, Inc. is an AREVA and Siemens company.

2.0 Historical Perspective

The cycle-specific DIVOM methodology is part of a long history that spans more than a decade of work by different organizations. In this section, the present effort is put into historical perspective as it relates to the Detect & Suppress (D&S) long term solution concept developed by the BWR Owners' Group (BWROG) and the BWROG sponsored work by the General Electric Company (GE). Fuel vendors other than GE have periodically participated at the invitation of the BWROG. The parallel independent work by FANP on DIVOM methodology is briefly covered here.

2.1 Brief History of BWROG and GE DIVOM Work

The US Nuclear Regulatory Commission (USNRC) and the BWROG began reevaluating the issue of instability and its consequences following the instability event at LaSalle Unit 2. Recognizing that the current reactor protection systems might not adequately prevent the violation of the safety limit minimum critical power ratio (SLMCPR) under oscillatory conditions, the BWROG launched a major campaign to develop long term solutions to assure compliance with the licensing criteria set forth in 10CFR50 Appendix A, GDC-12[†].

The long term solutions fall into two categories as detailed in Reference 1: region exclusion, and detect & suppress. This report is concerned with the latter solution (Stability Long Term Solution Option III D&S) as detailed in Reference 2, and its subsequent evolution.

---

† General Design Criterion 12 – Suppression of reactor power oscillations. The reactor core and associated coolant, control, and protection systems shall be designed to assure that power oscillations which can result in conditions exceeding specified acceptable fuel design limits are not possible or can be reliably and readily detected and suppressed.

2.1.1 Description of the Detect & Suppress Solution Option III

The D&S Option III solution depends on timely detection of oscillatory behavior by applying certain algorithms to the signals of several OPRMs[‡]. Any oscillation detection algorithm requires a delay time from the onset of oscillations to reliable recognition. In the case of the period-based detection algorithm (PBDA) used in the Option III application, the time delay is measured in the confirmation count, where 12~14 counts (6~7 oscillation cycles) are typically required to avoid spurious scrams. The timely suppression of the growing oscillation by scram, while assuring that the SLMCPR is not violated, depends on the following components of the methodology.

1. Determination of the minimum critical power ratio (MCPR) margin that exists prior to the onset of the oscillation. This is a plant- and cycle-specific calculation that determines the minimum expected MCPR based on specified scenarios, namely a two recirculation pump trip along the highest rod line and steady state operation at 45% flow and the highest licensed rod line.
2. Statistical calculation of the peak oscillation magnitude. This portion of the methodology is plant-specific and captures the effects of the plant specific trip system definition and setpoint on the magnitude of the hot channel power oscillation immediately before its suppression by scram.
3. The DIVOM curve. This is a conservative relationship between the fractional change in CPR and the hot channel power oscillation magnitude.

The selection of an OPRM setpoint per component (2) determines the hot channel oscillation magnitude (HCOM). The HCOM is transformed to a corresponding fractional change in CPR due to the oscillation using the DIVOM curve of component (3). Next, the fractional change in CPR due to the oscillation is used to assess the margin to the SLMCPR given the initial MCPR calculated in component (1). The optimum set point should be high enough to allow the PBDA sufficient time for reliable oscillation detection (i.e. an adequate number of confirmation counts), but must be low enough to preclude the violation of the MCPR safety limit. The determination of the set point is cycle-specific.

‡ OPRM (Oscillation Power Range Monitor) signal is a combination signal from a small number of closely-spaced Local Power Range Monitors (LPRMs).

2.1.2 The DIVOM Curve

The various components of the D&S solution described above and detailed in Reference 2, namely the OPRM design, the detection algorithm, the procedure for calculating initial MCPR, and the setpoint determination procedure, have reached a mature state. The notable exception is the DIVOM curve which is the focus of this report.

2.1.3 TRACG Generic DIVOM Curve

The first DIVOM curve was generated for the BWROG using the GE 3-D transient simulator code TRACG. In TRACG, fuel bundles were grouped into hydraulic channels according to their fuel type and oscillation magnitude, in addition to single (limiting) bundles simulated as individual channels. An event was simulated where unstable operation was reached (e.g. natural circulation), and growing oscillations are calculated. The calculated bundle transient thermal-hydraulic conditions are input to a bundle CPR evaluation tool. The time dependent power and CPR responses from TRACG are then processed to generate DIVOM: for each power oscillation peak, the normalized oscillation magnitude and the associated fractional change in CPR are determined. Thus, each TRACG analysis produces a set of points that can be used to obtain bundle-specific DIVOM curves. TRACG analyses (up to the time Reference 2 was issued) demonstrated that the DIVOM curve of the hot bundle was fairly linear and the thermal-hydraulic response to the oscillating power, represented by the slope of the DIVOM curve, could be conservatively bounded.

The TRACG calculations covered important variations of operating conditions and fuel parameters associated with all commercially available fuel types, including mixed fuel cores, and allowed the generic DIVOM curve (Reference 2), which bounds most of these calculations, to be validated on a generic basis (plant- and cycle-independent). The major qualitative difference in DIVOM behavior was found to depend on the oscillation mode, where the DIVOM curve for the regional mode shown in Figure 2-1 is nearly twice as steep as the DIVOM curve for the global mode shown in Figure 2-2.

2.1.3.1 Single Channel DIVOM for Other Vendors

As stated in Reference 2, *"Calculation of CPR response during an oscillation requires treatment of very complex neutronic/thermal-hydraulic phenomena. Explicit calculation of cycle-specific CPR response would, therefore, require sophisticated 3-D analysis techniques and entail expensive reload analysis."* In order to avoid burdening fuel vendors other than GE with the task of generating their own DIVOM curves based on full scope calculations, an effort was made to license the DIVOM curve generated by GE on a generic basis for all commercially available fuel types. However, uncertainties remained as to the validity of the generic curve for lead test assemblies and new fuel designs. A reduced scope DIVOM verification procedure was envisioned for other vendors based on a single channel standard problem. The D&S standard problem would consist of power and transient hydraulic boundary conditions from a TRACG calculation, which the respective vendor, with its own fuel design parameters and CPR correlation (e.g. using XCOBRA-T in the case of FANP), would use to drive a single channel model.

The concept of the single channel standard problem failed due to the lack of understanding, at the time of its proposal, of the physical mechanisms behind the marked difference in the DIVOM slope between a global and a regional oscillation event.

2.1.3.2 Generic DIVOM is Potentially Non-Conservative

In June 2001, an initial report (also referenced in the final report Reference 3) to the NRC under 10 CFR part 21 (d) was filed (See Reference 4). Evaluations by GE identified a non-conservative deficiency in the generic DIVOM curve specified in Reference 2. Specifically, the regional mode DIVOM slopes could be significantly higher than the licensed generic curve for conditions of high bundle power-to-flow ratios. Similar observations were found for the global mode DIVOM under conditions of high core power-to-flow ratios.

As an interim fix to the problem, GE provided the affected utilities with a Figure of Merit (FOM) correction to the generic DIVOM slope, where the FOM is derived on either a generic or plant-specific basis. The FOM is an empirical concept based on TRACG experience and is intended to provide conservatism for high power-to-flow cases (functionally dependent on peak bundle power-to-flow ratio for the regional mode and core power-to-flow ratio for the global mode).

2.1.3.3 Resolution of Part 21 with Cycle-Specific DIVOM

Following the issue of the 10CFR21 report, the OPRM trip function remained unarmed, or was declared inoperable. The main reason was the potential for the system to trip the plant upon false identification of unstable oscillations if the setpoint was set unnecessarily low. The probability of such spurious scrams was increased with the low trip setpoints necessitated by a high DIVOM slope resulting from the FOM correction.

The BWROG Detect and Suppress Methodology Committee, which re-formed to address the Part 21 challenge, concluded that the best resolution of the potentially non-conservative DIVOM issue was to eliminate the generic DIVOM curve and substitute a cycle-specific DIVOM analysis in the approved Option III framework (See Reference 5).

2.2 History of DIVOM Calculations at FANP

The DIVOM work by GE, sponsored by the BWROG, was paralleled at FANP with a somewhat reduced scope and time delay. The purpose of the FANP work was motivated by the need to confirm the GE results and their applicability to FANP fuel. This work had to be independent from that of the BWROG as the single channel standard problem concept failed to materialize. Without the standard problem, the DIVOM curve generated by TRACG and the GE dryout correlation GEXL had to be coupled with the rest of the reload review in which the FANP dryout correlation is used. While the assumption that such methodology differences are negligible has been confirmed, it was felt at that time that the methodology gap between BWROG and FANP was a weak point in the D&S methodology applications at FANP, and in-house independent verification was needed. In addition, new fuel designs at FANP would require validation and, at least, a rudimentary in-house capability for calculating DIVOM curves would be required.

In the next two sections, two DIVOM methodologies developed at FANP are presented briefly.

2.2.1 DIVOM Work with RAMONA3 System Code

The DIVOM calculation capability requires two main pieces: a transient system code capable of simulating regional mode oscillations and a dryout correlation to calculate the hot bundle response to the power oscillations. For the first piece, the Studsvik-Scandpower code RAMONA3 (Reference 6) was readily available and good experience with it had been accumulated at Framatome ANP in Germany.

The ANFB dryout correlation, which is licensed for application in the US, was programmed in the RAMONA3 code to create a tool for DIVOM verification. Several cases were simulated for global oscillations in a 648 bundle core, and regional oscillations in a 784 bundle core. Cores made up of 9×9 fuel, ATRIUM-10 fuel, and mixed fuel cores were analyzed. The DIVOM results are reproduced here as Figure 2-3 and Figure 2-4 for the regional and global DIVOM respectively. The similarity of the RAMONA3 DIVOM calculations shown in Figure 2-3 and Figure 2-4 with those of Figure 2-1 and Figure 2-2 calculated by TRACG is remarkable[§].

While this study was limited in scope, it did support the generic validity of the BWROG DIVOM curve and established the RAMONA3 code as an appropriate tool for evaluation of new fuel designs.

2.2.2 DIVOM Work with XCT-MODES Single Channel Code

The scope of the RAMONA3 study was limited by the labor intensive process for generating neutronic input and the computer time for the full 3-D analysis. In addition, the analysis often encountered difficulties due to developing undesired oscillation modes necessitating an iterative search for parameters like control rod patterns that would exhibit the desired mode of oscillation. In contrast, the theoretical work to make the DIVOM curve calculation possible with a single channel had matured since it was first mentioned in Reference 7. The key to successful single channel DIVOM calculations that properly distinguish between the global and regional modes turned out to be the application of 3-D modal neutron kinetics instead of nodal 3-D methods. A single channel model was created using the FANP 1-D transient thermal-hydraulic code XCOBRA-T (Reference 8) coupled to a new modal kinetics module.

The XCT-MODES method was distinguished with the following features:

- The application of modal neutron kinetics. This allowed direct accounting of the oscillation mode through the subcritical reactivity parameter. Sensitivity of the DIVOM slope to the subcritical reactivity could be quantified, while it could be

§ Minor differences exist between the two DIVOM sets. For the global mode, the RAMONA3 DIVOM curve does not require a shifted line implying finite CPR response to zero oscillation magnitude, perhaps to fit one of the TRACG global cases which seems to have a larger slope than the rest. For the regional mode, all of the RAMONA3 cases lie conservatively below the 0.45 slope DIVOM line.

previously studied only through variations of parameters such as control rod patterns and core size.

- The application of a single channel representing the hot channel. [

]

- Instead of a closed loop model simulating the growing instability, the kinematics of the oscillation was simulated by an open loop model. Specifically, a growing inlet mass flow rate oscillation was imposed as a boundary condition to the hot channel. This proved very useful to avoid issues such as numerical diffusion and their dampening effect in codes such as XCOBRA-T, and allowed the variation of important parameters such as oscillation frequency which could not be varied in full system simulations.

The XCT-MODES code was used to perform an extensive study with wide variations of parameters. These parameters included:

1. The oscillation mode (global versus regional)
2. Void-reactivity coefficient
3. Subcritical reactivity
4. Oscillation frequency
5. Oscillation growth rate
6. Hot bundle power
7. Hot bundle mass flow rate
8. Inlet subcooling
9. Fuel conduction time constant (gap coefficient)
10. Fuel design (ATRIUM-9B and ATRIUM-10)
11. The critical heat flux (CHF) correlation (SPCB, ANFB-10, and ANFB)
12. Local rod power peaking factor, as change of F-effective in CHF correlations

The resulting DIVOM curve set for the regional and global modes, reproduced here as Figure 2-5 and Figure 2-6 respectively, were found to be remarkably similar to those of TRACG (Figure 2-1 and Figure 2-2) and RAMONA3 (Figure 2-3 and Figure 2-4).

The main drawback of the XCT-MODES method was [

] This led to the failure of the method to provide explanation or resolution of the Part 21 issue regarding the elevated DIVOM slope with high power-to-flow ratios as reported by GE.

2.2.3 FANP Review of Part 21 Issues

An extensive study of the Part 21 issue was conducted in preparation for the cycle-specific DIVOM project, which was aimed at evaluating the possible causes of the elevated DIVOM slope reported by GE. [

]

[

]

2.2.4 Present RAMONA5-FA DIVOM Methodology in Perspective

The transient system code used for the present DIVOM methodology [ ] The most significant points are given below.

- The base code is the system code RAMONA5, which is a complete 3-D transient system code version. It is the latest version following RAMONA3 used in the first DIVOM verification study.
- The neutron cross section data and hydraulic core data [ ]
- The differences in initial steady state power distribution between the steady state simulator and the transient code [ ]
- [ ]
- The fuel pin model in RAMONA was improved [ ]
  - Account for fuel pellet conductivity dependence on temperature and exposure
  - Detailed gap conductance model
  - Account for neutron self-shielding effects on power deposition distribution in pellets.
- FANP hydraulic and dryout correlations have been installed.

The new code version, RAMONA5-FA, is the center piece of the methodology for DIVOM calculations at FANP, consistent with the BWROG requirements.

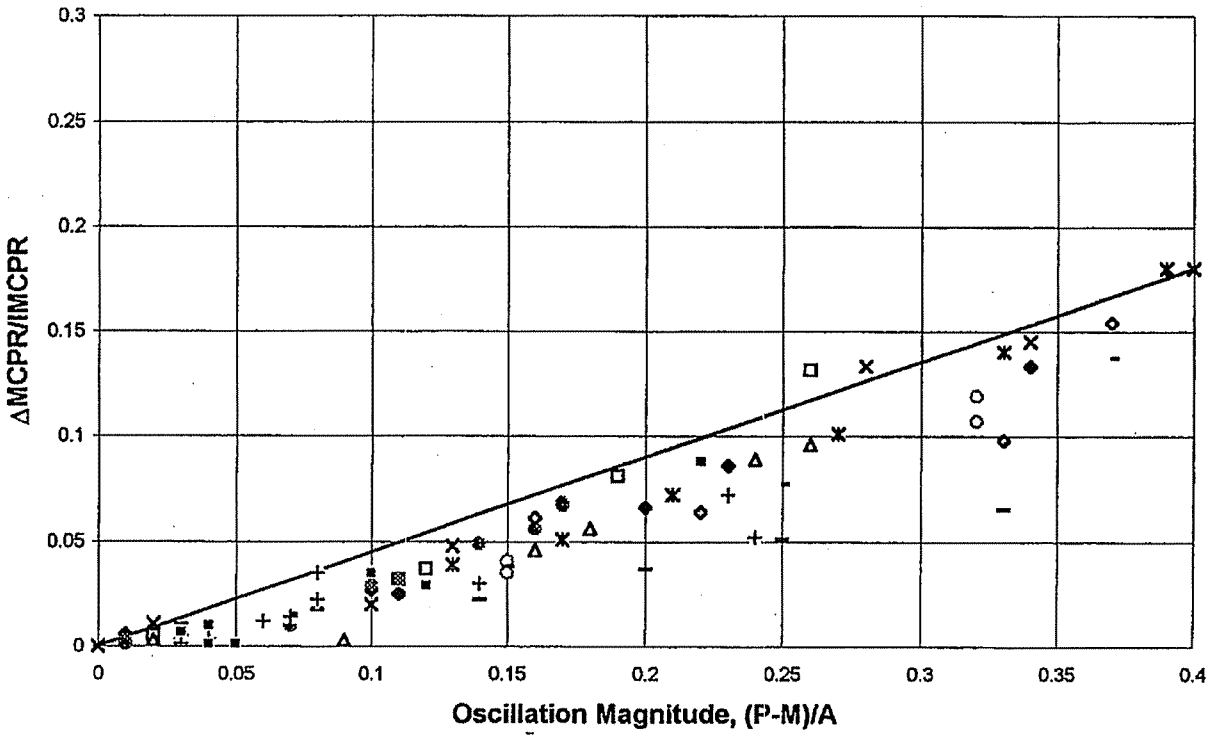

Figure 2-1 GE Generic Regional Mode DIVOM Curve

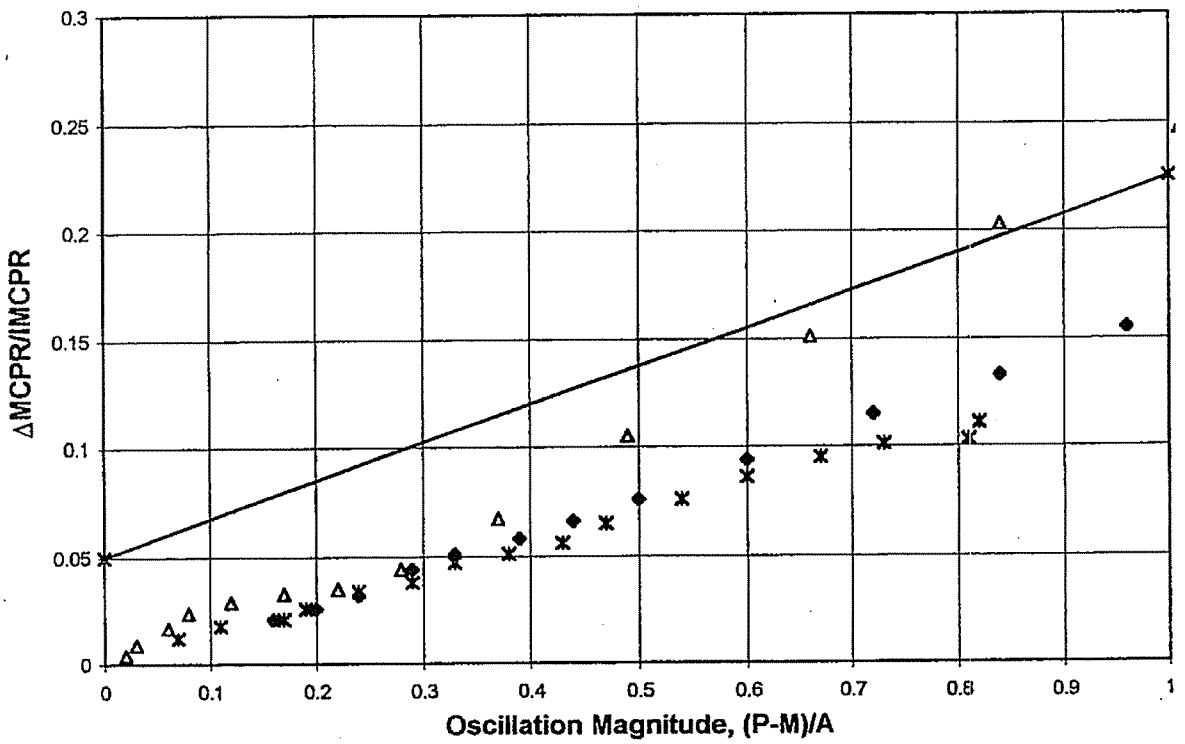

Figure 2-2 GE Generic Global Mode DIVOM Curve

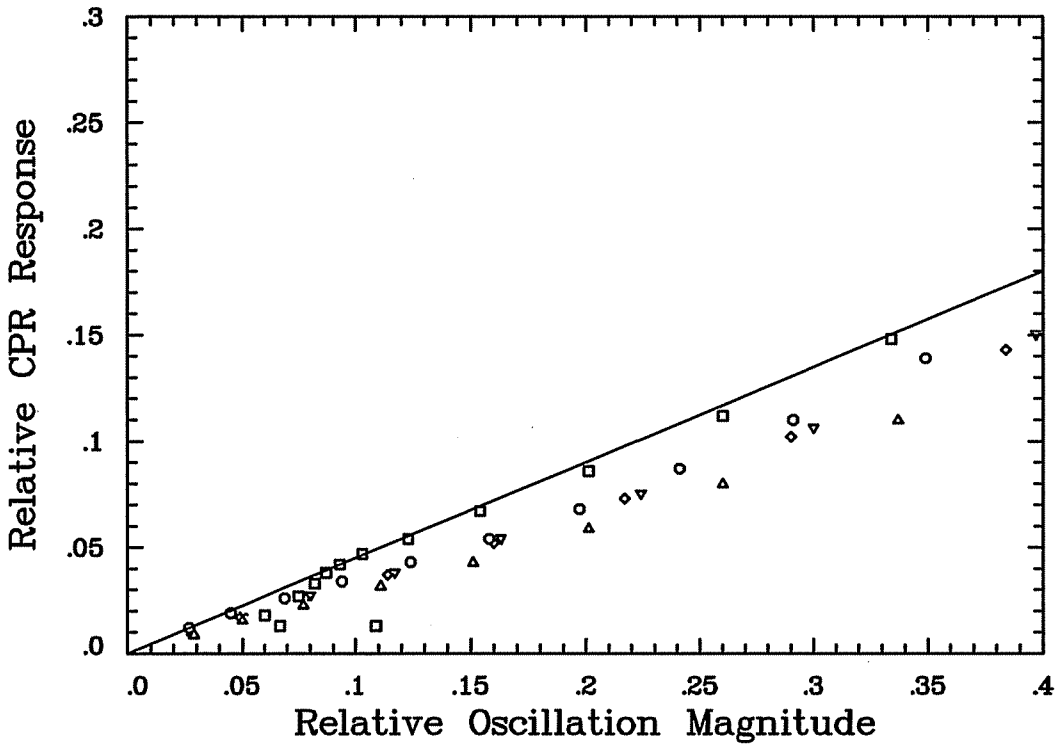

Figure 2-3 FANP RAMONA3 Regional Mode DIVOM Curve

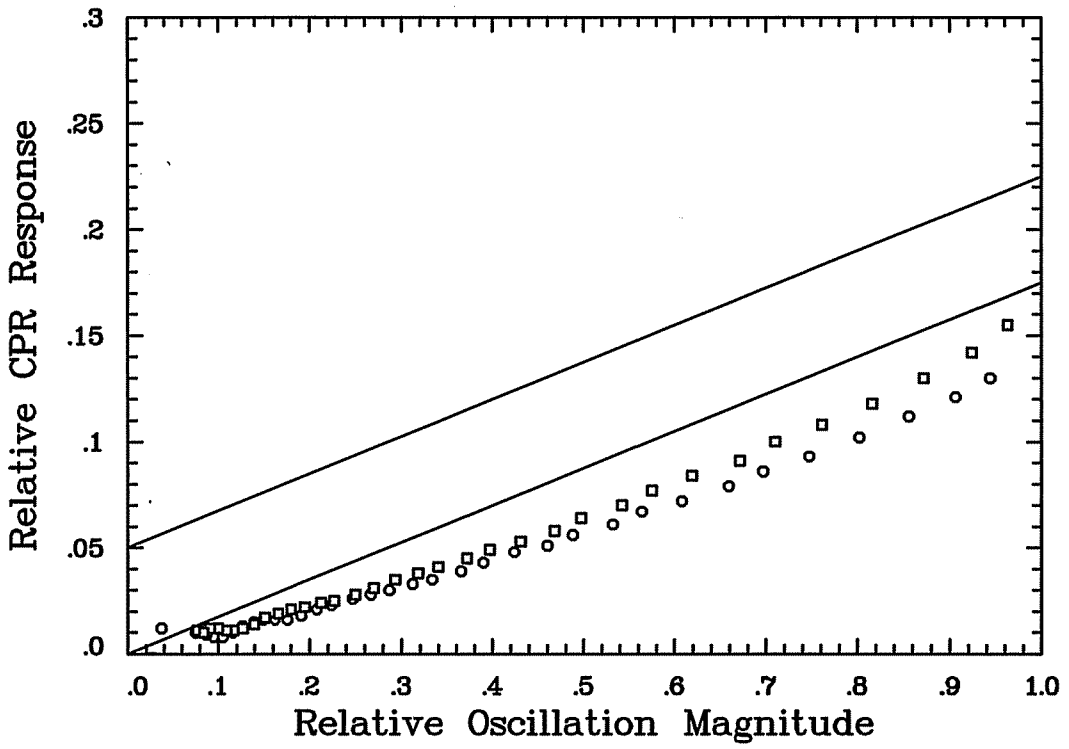

Figure 2-4 FANP RAMONA3 Global Mode DIVOM Curve

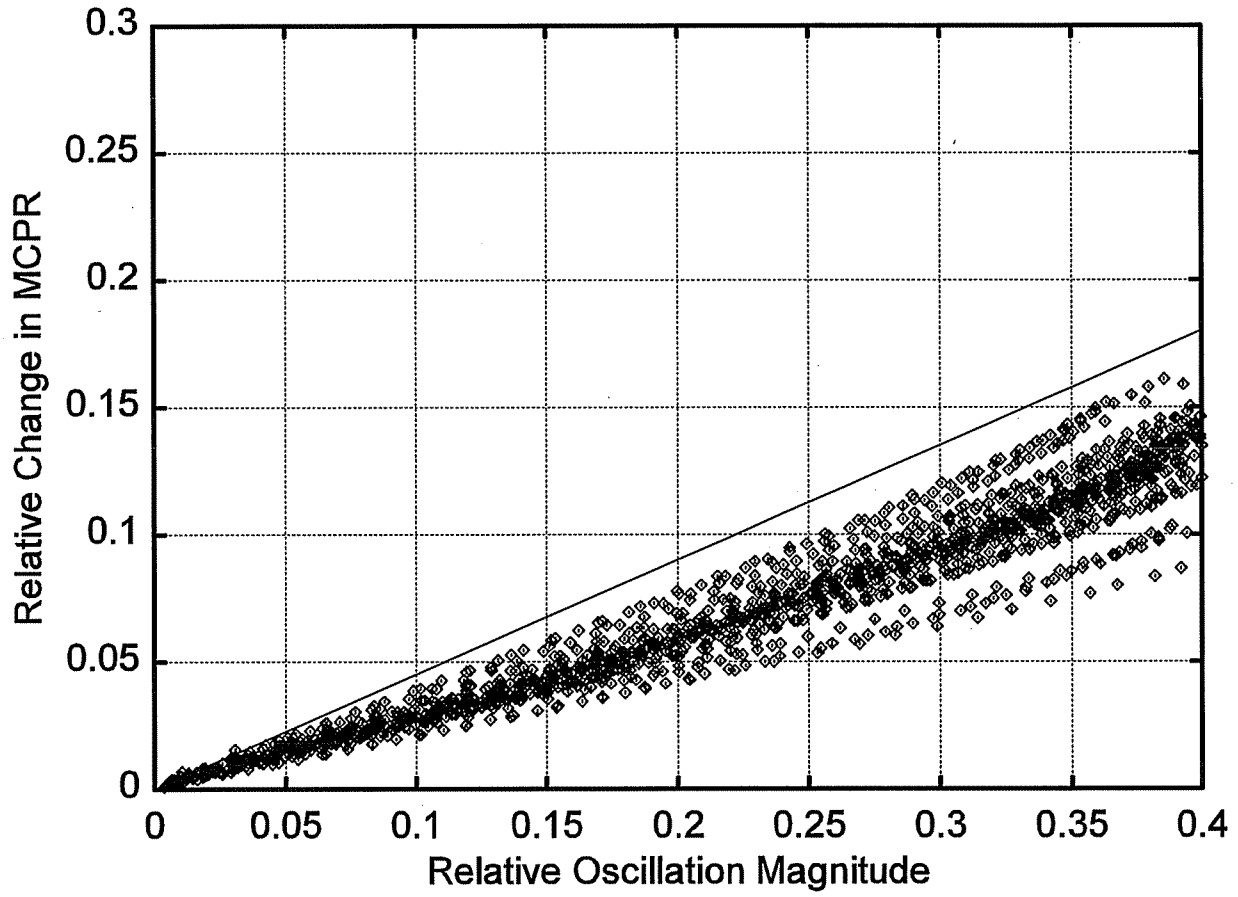

Figure 2-5 FANP XCT-MODES Regional Mode DIVOM Curve

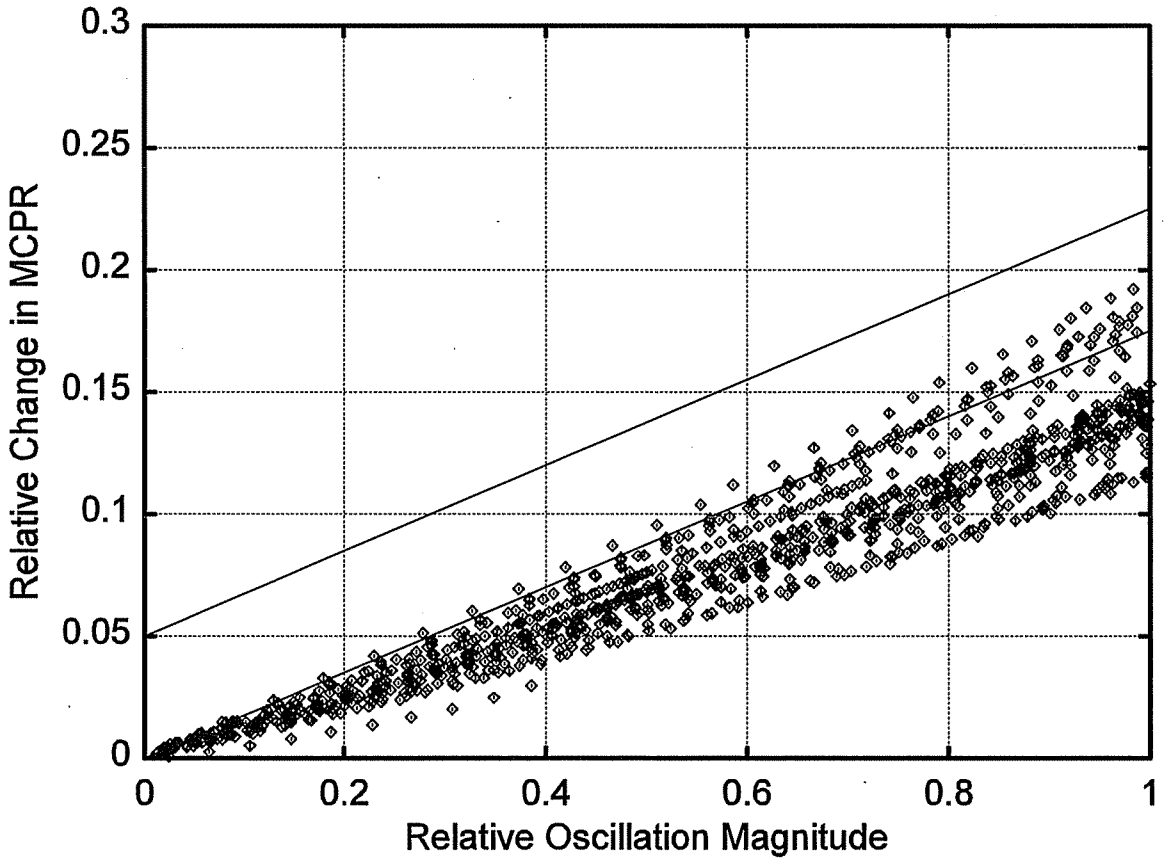

Figure 2-6 FANP XCT-MODES Global Mode DIVOM Curve

3.0 The Physical Phenomena Pertinent to a DIVOM Calculation

In this section, an integral review of the basic physical phenomena is presented. These can be divided into the phenomena leading to power and flow oscillations, and the dryout phenomena under these oscillatory conditions. The reason for this division is that the dryout phenomena do not feedback to the mechanisms influencing the nature of the oscillation.

3.1 Power Oscillation Phenomena

The power oscillations that may occur in a BWR result from the complex interaction of many physical processes related to fluid flow, convective and conductive heat transfer, and nuclear reactivity. Although all the related phenomena are modeled to a high degree of detail in a large system code like RAMONA5-FA making it capable of simulating the resulting oscillations, it is helpful to demonstrate basic understanding of the underlying processes and their interaction. In particular, this understanding leads to the conceptual separation between the dynamics of the oscillations which is generally sensitive to modeling biases and the kinematical descriptive side which is less sensitive to modeling biases. Study of the system dynamics provides full information about the system and its stability (decay or growth ratio and frequency of oscillations). The kinematical aspect is related to the description of the system variables relative to each other regardless of its degree of stability and is important for calculating the DIVOM response.

3.1.1 Hydraulic Density Waves

The central phenomenon is the density wave in a heated, vertical, boiling channel such as a BWR bundle. For a given flow perturbation at the channel inlet, given the same energy transfer, a corresponding change in the void fraction (density) takes place. This change in density travels upward with the flow as a packet hence the term "density wave." The inlet flow perturbation can take any functional form, which can be linearly decomposed into sinusoidal waves of different magnitudes and frequencies. A sinusoidal perturbation is therefore the basic form of the time variation of the wave parameters as long as the magnitudes of these parameters remain sufficiently small for linearity to remain valid.

In describing the hydraulic density wave kinematics in a heated channel, there was no reference to a preferred oscillation frequency nor to whether an initial perturbation will grow or decay, i.e. its stability. The determination of the stability of a density wave is accomplished by studying its dynamics, i.e. the feedback mechanisms that affect the original perturbation. In this particular case, the idealized boiling channel is assumed to have an imposed constant pressure drop boundary condition. An inlet flow perturbation creates corresponding density and mass flux fluctuations with the same frequency but with an associated phase lag (time delay) as they propagate upward. The variation in density results in gravitational head change, while the mass flux variation results in friction variations. The net pressure variation across the channel due to the gravitational and frictional components must be compensated for by flow acceleration in order to satisfy the net constant pressure difference boundary condition. Now, the importance of the frequency of the oscillation is evident as it affects the phase of the flow acceleration relative to that of the initial flow perturbation. The frequency that results in a phase difference of typically 180 degrees between the inlet and exit flow is the limiting frequency that receives the maximum amplification.

The inlet flow oscillation with the preferred frequency may grow in time (unstable) only if the degree of amplification from the pressure drop is large enough to overcome the frictional dissipation. The quantitative parameter for measuring the degree of stability is the decay ratio defined as the oscillation magnitude at a given cycle relative to the previous cycle's magnitude. Under typical BWR conditions, the decay ratio is increased (less stable) with the following system variables:

- High power to flow ratio: This increases the density contrast along the channel (and hence the gravity head) which drives the instability.
- Low flow: In addition to being the denominator in the power-to-flow ratio, low flow is destabilizing because it decreases the preferred frequency (because lower flow speed reduces bubble transit time) and thus reduces the axial attenuation of the mass flux and void fraction.
- Bottom-skewed power peaking: This results in creating the bubbles at lower elevations which remain for a longer time, thus increasing the average density contrast and thus is destabilizing.

- Low system pressure: Low system pressure is destabilizing as the difference in saturated liquid and vapor densities increases which drives the gravitational component, hence a destabilizing effect.

- Upward friction distribution shift: Friction plays two competing effects. On one hand, friction is stabilizing as it dissipates the oscillation energy. On the other hand, the friction component in the upper part of the channel (which is time lagged compared with the single phase region at the inlet) is part of the delayed pressure drop that drives the instability. Thus, high friction in the upper part of the channel combined with low friction in the lower part of the channel results in a maximum destabilization effect. The actual picture is rather complex, for moving a local friction pressure drop device such as a spacer upward in a rod bundle will increase its destabilizing effect due to the increased time lag but it also reduces its effect as the mass flux it experiences is attenuated further. A simplified representation of the destabilizing effect of the up-skewed friction distribution is commonly expressed in terms of the two-phase-to-single-phase pressure drop ratio.

Important results that emanate from the previous discussion are listed below.

1. The oscillation dynamics are important in determining the correct frequency. [

   ]

2. The decay ratio [

   ]

3. Input biases affecting the friction distribution will change the decay ratio [

   ]

The idealized picture of density waves presented above will be integrated in the real BWR environment where other feedback mechanisms play important roles. These are discussed in the next sections.

3.1.2 Neutron Kinetics

The water flowing up the boiling channels in a BWR plays a dual role: a coolant and a neutron moderator. The variation of the water density due to density waves alters the nuclear cross sections at the location of the respective density change. Density-reactivity coefficients vary from one fuel design to another and are different at different densities, making detailed simulation necessary. In this section, the major trends and effects of the neutron kinetics are discussed which will aid in understanding the trends of the detailed simulations.

The reactivity changes due to the density wave are translated into fission power changes, which provide feedback into the energy balance of the channel and affect its stability. The magnitude and phase of the feedback are important to determine its destabilization effect. The feedback of the fission power to the channel energy balance is filtered through the fuel pin conduction.

At conditions of relatively high power-to-flow ratios associated with unstable behavior, the void content is high and the relative power is therefore pushed down to lower elevations. The bottom-skewed axial power shape is destabilizing as was discussed earlier, because it increases the density contrast in the channel. At the same time, the axial power shape impacts the magnitude of the reactivity response. The net reactivity change is obtained by weighting the local reactivity perturbation with the neutron importance function, where the latter is proportional to the square of the neutron flux shape. As the power is generally proportional to neutron flux, bottom-skewed power shapes result in higher weighting of the bottom part where the reactivity changes are small, hence resulting in a reduced density-reactivity feedback which is stabilizing. Thus, there are two competing effects of the down-skewed axial power shape – destabilizing for the hydraulics, and stabilizing for the neutronic feedback. The net effect on the coupled system is generally destabilizing, resulting in increased decay ratio. [

]

[

]

3.1.3 Fuel Pin Heat Transfer

A small fraction (2 ~ 3%) of the fission energy is deposited directly (and almost instantaneously) in the coolant. An initial density change results in an instantaneous reactivity change, while a reactivity change will result in fission power response with a significant phase lag of nearly 90 degrees due to the effect of the delayed neutron precursor decay. The direct energy deposition perturbation results in instantaneous evaporation rate response (no phase lag), which produces a density response which lags the energy deposition perturbation by another 90 degrees. The resulting 180 degree lag (out-of-phase) effect of the reactivity-to-direct energy deposition transfer function is stabilizing. Its effect on decay ratio can be significant (See Reference 10). However, the difference between a detailed nodal representation and a core average energy deposition fraction is small.

The bulk of the fission energy is deposited in the fuel pins. The fluctuating component of the heat deposited in the fuel pins is significantly damped by the time it reaches the cladding surface. The degree of damping is increased with the heat capacity and pin diameter, and decreases with thermal conductivity and fuel-clad gap conductance. The pin heat transfer time constant can be approximated from:

$$\tau = \rho_f C_p \left(\frac{D^2}{32\kappa_f} + \frac{D}{4h_{gap}} \right)$$

where ρ_f is the fuel pellet density, C_p is its specific heat, κ_f is fuel conductivity, h_{gap} is the pellet-clad gap conductance, and D is the pin diameter. Time constants of the order of 2 ~ 4 seconds cover the expected range of current fuel designs. However, it should be noted that the actual effective time constant also depends on the radial distribution of the heat deposition in the pellets. For higher energy deposition near the surface of the pellet, the effective thermal diffusion length is decreased thus decreasing the effective time constant.

The time variation of the energy transferred to the coolant through the clad surface heat flux is a filtered response of the fission energy deposition with the filter time constant given above. Significant damping of the order of

$$\xi = \frac{1}{\sqrt{1+\omega^2\tau^2}}$$

results, where $\omega = 2\pi f$ is the frequency in radians per second and f is frequency in Hz. The magnitude of the heat flux response is typically 8 ~ 12% of the originating heat generation perturbation. The corresponding phase shift is:

$$\theta = \tan^{-1}(\omega\tau)$$

This means that the phase difference between the direct energy deposition in the coolant and the component of energy addition through heat flux at the clad surface is significant. These two components need to be modeled in detail, [

]

A bias which increases the gap conductance reduces the fuel time constant and increases the decay ratio. [

]

3.1.4 Oscillation Modes

In the above sections, the discussion of the oscillation phenomena focused on an idealized single channel. In this section, the discussion of the phenomena is generalized to include

parallel channels in a BWR core. Different oscillation modes are possible depending on the flow redistribution pattern between the parallel channels and the excited spatial neutron flux mode.

3.1.4.1 The Global Mode

In this mode, all the bundles in the core oscillate coherently in phase. The ensemble of parallel channels behave qualitatively like a single channel, and accounting for individual channels is necessary only for the resolution of radial power peaking effects.

The recirculation loop flow and pressure drop must match those of the core. In that way, the characteristics of the recirculation loop (hydraulic resistances, inertia, and pump curves) influence the stability of the global mode.

The propagation of density waves through all the core channels results in net reactivity oscillations. [

]

[

]

3.1.4.2 The Regional Mode

The regional mode is characterized with half the core bundles oscillating out-of-phase with the other half. The net core flow remains unchanged during the regional oscillation provided its magnitude is not so large as to introduce nonlinear effects that do not cancel out.

The main reason the hydraulic channels prefer to oscillate out-of-phase is the cancellation of the recirculation loop damping. The regional mode oscillation in a BWR is forced to be coherent with half the core bundles oscillating in-phase and the other half oscillating with a 180 degree shift due to neutronics coupling. The half-core oscillation is preferred because it excites the first azimuthal neutron flux mode and thus receives the highest possible amplification. The other flux harmonics that can be excited by other channel groupings are characterized by large subcritical reactivities, and therefore are significantly damped.

In the description above, it is shown that the regional oscillation excites the first azimuthal flux harmonic, and its neutral line of symmetry divides the core into two halves where the density wave oscillations are in-phase in each core half and out-of-phase with each other.

The simulation of a regional mode oscillation requires the ability to account for neutron flux shape changes as a function of time. Experimental and theoretical studies (See References 12 and 13) corroborate to confirm that the first azimuthal mode is excited and can be extracted by an orthogonalization process from the oscillating power shape. [

]

It is important to notice that the decay ratios of the regional and global modes are comparable. As shown in Reference 14, the regional mode is preferred for

- Large cores, which result in small eigenvalue separation for the first azimuthal flux mode.

- Low center power peaking (ring of fire), which also decreases the eigenvalue separation.

- Loose inlet orifice, which destabilize the hydraulic channels. This effect favors the regional mode in the absence of recirculation loop damping. It must be emphasized [

.]

The effect on the DIVOM curve is dominated by the first harmonic eigenvalue separation. As shown in Reference 11, the neutronic response of the harmonic power relative to that of the fundamental mode, given the same reactivity input, is obtained from:

$$\frac{\Delta P_{Harmonic}}{\Delta P_{Fundamental}} = \frac{1}{1 + \Delta\rho_{Harmonic}}$$

which explains why the DIVOM curve for the regional mode is limiting. [

]

3.1.4.3 The Rotational Mode

In the regional oscillations described above, the neutral symmetry line is stationary. The rotational mode is similar to the regional mode where the neutral line is oscillating or rotating (See Reference 13). The rotational mode essentially results from the simultaneous excitation of two orthogonal azimuthal modes. Assuming the core loading and control rod patterns are symmetric, the first two azimuthal modes are degenerate (approximately equal eigenvalues),

and are thus indistinguishable. [

]

3.1.4.4 The Neutron-Uncoupled Channel Mode

The discussion of density waves was idealized as occurring in a single channel under constant pressure drop boundary condition, then generalized to coupling with the neutronic feedback to get to the prevailing oscillation modes in a BWR. It must be noted that the idealized single channel oscillation may still occur in a BWR core under certain conditions. The nature and effects of single channel oscillations on DIVOM results are presented in this section in order to show that, while such effects are relatively small in typical situations, they are not neglected in the present methodology.

Any density wave in a single channel can be accurately assumed to occur under constant boundary pressure, as the impact of the out-of-phase oscillation required by the rest of the core on the core pressure drop will be imperceptibly small. The single channel density variations are too small to significantly excite neutron responses and the core power response will remain dominated by the coherent many channel oscillations. In that way, the idealized situation is realized: single channel under constant pressure drop without nuclear feedback.

The channel decay ratio is usually smaller than the global or regional decay ratio and single channel oscillations may occur only under rare situations**.

** Examples for single channel oscillations in actual BWR experience are rare. In one occasion, channel instability occurred because of high exit resistance in a particular channel due to instrumenting it with a turbine flow meter. Another example is the unseated bundles in Forsmark.

It is important to notice that although the channel decay ratio is normally lower than the decay ratio for the global and regional modes, unstable single channels are possible when the reactor is brought far into unstable operating conditions. In that manner, all decay ratios (regional, global, and channel) are higher than unity. These situations may occur in DIVOM calculations for high power-to-flow ratios, and is expected to occur more often for plants with power uprate and extended load lines.

[

]

3.1.5 Non-Linear Effects

The DIVOM calculation is normally extended to include relatively large oscillation magnitudes. The nonlinear effects become noticeable at such oscillation magnitudes. The nonlinear effects are intrinsically accounted for in a large system code like RAMONA5-FA. Some of these nonlinear effects can be deduced from simple theory and confirmed by code calculations and reactor measurements. Some of the nonlinear effects are mentioned here.

3.1.5.1 Limit Cycles

Unstable oscillations grow exponentially from a small perturbation. As the oscillation magnitude increases, nonlinear effects come into play, which dampen the system (supercritical Hopf bifurcation). A stable limit cycle eventually develops where a finite oscillation magnitude is reached and the magnitude of the limit cycle is proportional to the degree of linear instability.

It was shown in Reference 15 that the saturation of the growing oscillation into a stable limit cycle occurs because of the negative reactivity bias that results from the reactivity oscillation. In Reference 7, it was shown that the regional mode reactivity bias due to oscillation is smaller (nearly half) that of the global mode, and therefore a regional power oscillation is expected to grow to larger magnitude limit cycles than the global oscillation.

A single channel oscillation under constant pressure drop and no power feedback also experiences nonlinear effects, but the flow oscillations tend to grow to large magnitudes before saturating into a limit cycle.

3.1.5.2 The Double Frequency Global Component

The growth of the first azimuthal power oscillations was shown in Reference 7 to excite a global component with double the frequency of the original regional oscillation. This does not mean that the global mode has become unstable, but simply driven by the nonlinear regional oscillation.

The presence of a global component also excites corresponding global (net core) flow and pressure drop components which interact with the recirculation loop.

This double frequency global component is noticeable near the end of a typical DIVOM transient as expected, [

]

3.1.5.3 Nonlinear Coupling to Single Channel Oscillations

The possibility of single channel oscillations being uncoupled from the neutron feedback has been discussed earlier. The decoupling between the neutronic power and the density wave in a single channel originates in the small effect of a single channel density perturbation on the whole core behavior, and also in the frequency of the power oscillation which is different from that of the single channel. [

]

3.1.5.4 Subcritical Hopf Bifurcations

Hopf bifurcations with regard to BWR oscillations are discussed in detail in Reference 16. Essentially, a subcritical Hopf bifurcation results in a linearly-stable BWR experiencing growing oscillations when excited by a large magnitude perturbation. The occurrence of subcritical Hopf bifurcations in a BWR is rare, and was demonstrated in Reference 16 in one instance and calculated using the common version of the RAMONA code. [

]

3.2 Dryout Phenomena

The second part of the DIVOM calculation is the capability to quantify the CPR at any time throughout the regional oscillation transient. The transient system code provides the thermal-hydraulic parameters required by the dryout correlations to calculate CPR. This section is devoted to the dryout phenomena and how they are represented by the correlations in an instability oscillation.

3.2.1 Steady State Dryout Correlations

The dryout correlations are basically steady state formulae which are fitted for specific fuel types to steady state dryout data representing anticipated operating conditions in a BWR.

There are two correlation types in common use. The first one is based on the critical heat flux (CHF) concept, e.g. XN, ANFB, ANFB-10, and SPCB correlations used at FANP in the United States. The second type is based on the critical quality versus boiling length (XL) concept, examples of which are the KWUXL9 and KWUXL10 series of correlations used by FANP in Germany and GEXL correlation at GE.

3.2.1.1 General Description of CHF Correlations

The critical heat flux is expressed empirically as a function of the planar enthalpy at the boiling transition elevation, where the unknown coefficients are generally dependent on mass flux and pressure for a specific fuel bundle type. Corrections for pin power distribution and axial power shape are important parts of a CHF correlation. The unknown coefficients must be fitted to test data to make it applicable for a specific fuel design.

Dryout test data are collected using electrically heated full scale bundles for a wide range of operating conditions (flow rate, inlet subcooling, and pressure). Different bundles of the same type are tested with variations in axial power peaking and radial pin power distributions. For a given test run, the power is increased slowly until indications of dryout are registered as a sudden rise in pin temperature for any pin at any elevation.

While the licensing applications define thermal margins based on critical power ratio (CPR), CHF correlations are set up to calculate the critical heat flux ratio (CHFR) defined as the ratio of the critical to actual heat flux. Dryout is indicated when the minimum critical heat flux ratio (CHFRMIN) reaches unity. In order to calculate CPR, an iterative process is necessary where the power is increased (or decreased), while keeping all other parameters unchanged, until CHFRMIN=1 is calculated. The increase of power in this calculation results in increasing the planar enthalpy and decreasing the critical heat flux, while the actual heat flux is increased, bringing the CHFRMIN closer to unity. CPR is defined as the factor that must be used to multiply the actual bundle power to get CHFRMIN=1. In that manner, for conditions where

margin exists, we always find that CHFRMIN > CPR > 1. The two parameters are equal only at the critical conditions.

3.2.1.2 General Description of XL Correlations

Although dryout correlations licensed in the US for use by FANP are all of the CHF type, some consideration of the behavior of the XL correlation form is appropriate given the fact that the original DIVOM methodology and the generic DIVOM curve were developed using GEXL.

Instead of critical heat flux, the XL correlations are based on correlating critical quality. Instead of using planar enthalpy as the independent parameter, the XL type uses the equilibrium boiling length defined as the length of the two-phase section up to the elevation of interest. Dryout is indicated when the actual equilibrium quality reaches the critical quality calculated by the correlation at any elevation. Radial corrections for pin power distribution are also part of the XL correlation, and the unknown coefficients of the XL relationship are fitted to test data similar to the case of CHF correlations.

Similar to CHF correlations, the XL type correlations do not calculate CPR directly. Instead, a quantity defined as thermal margin (TM) is directly calculated and is defined as the ratio of critical to actual quality. Dryout is indicated when the minimum thermal margin (TMMIN) at any elevation is reached. An iterative process on power is required to search for the power multiplier (the CPR) that brings TMMIN to unity, a similar procedure described above for CHF correlations.

[

]

3.2.2 Application of Dryout Correlations to Oscillatory Conditions

There are two main issues regarding the application of steady state dryout correlations under oscillatory conditions. The first is the applicability of the CPR concept under transient conditions. The second issue is the inherent conservatism when a steady state correlation is applied to transient conditions.

When the concept of CPR was introduced, it was considered more convenient and descriptive from the operations point of view as it relates directly to the power margin. The more physical concept of CHFR is not as transparent in giving indication of margin as power increase would simultaneously alter both heat flux and critical heat flux. The problem is that the CPR is not rigorously defined under transient conditions.

In the case of XL correlations, the instantaneous boiling length can be calculated and the critical quality can be inferred by applying the correlation. In doing so, an implied assumption is that the conditions that altered the bottom location of the boiling inception result in instantaneous impact downstream. In order to avoid difficulties of that nature, the transient CPR is defined assuming that the thermal margin (TM) can be calculated based on instantaneous conditions (quasi-steady state), and that the relationship between TM and CPR is linear and remains constant at the initial steady state conditions.

The case of the CHF correlation application to transient conditions is slightly less problematic. The CHF can be calculated based on instantaneous local conditions with the necessary assumption that the axial power shape correction is instantaneously applicable. The main assumption under transient conditions is that during the power iteration process to calculate CPR, the instantaneous shape of the axial enthalpy distribution is maintained. This assumption is strictly valid only for quasi-steady state conditions.

Fortunately, in the case of DIVOM analysis, we have two well-defined CPR points. The first point is the initial steady state. The second point is the last point where CPR=1 is reached for most cases. The last point with CPR=1 is characterized by CHFRMIN=1 in the case of CHF correlation and TMMIN=1 in the case of the XL correlation. With CHFR and TM being better defined under transient conditions than CPR, the last point is therefore well defined. The cyclical minimum CPR points that occur between the two well-defined end points have been shown to vary smoothly, which is the basis for accepting the transient CPR concept under oscillatory conditions regardless of the correlation used.

It remains to discuss briefly the conservatism inherent in applying the steady state dryout correlations to transient conditions. Dryout can be defined as the loss of liquid film which causes a sharp decrease in heat transfer coefficient. Prior to dryout, the liquid film mass balance is maintained between evaporation due to heat flux and droplet deposition which is

inversely proportional to quality (or equivalently mixture enthalpy). [

]

The small conservatism discussed above is approximately offset by a small non-conservative input to the correlation related to the attenuation of density waves. It is known that a propagating density wave is attenuated as it travels upward in a boiling channel. That means that the mass flow oscillation magnitude at the inlet is significantly larger than its value near the top of the boiling channel which is the limiting elevation for dryout. The damped flow rate at the top elevation is responsible for similarly damped quality and enthalpy oscillations which are used as input to the dryout correlations of the XL and CHF type respectively. This attenuation is physical, but it is normally augmented by a small component due to numerical diffusion when calculated by transient codes. The small component of numerical diffusion results in corresponding overestimation of the inlet mass flow oscillation magnitude and underestimation at the top of the bundle. The numerical diffusion, [

], is responsible for the small non-conservative input to the dryout correlation.

The effect of the small non-conservative input to the dryout correlation due to the numerical diffusion component of the density wave attenuation is examined by comparing RAMONA5-FA results to test data [

] These comparisons are discussed in the next section, and show good predictive capability of the RAMONA5-FA code and dryout correlations under oscillatory conditions.

3.2.3 Comparison of Dryout Correlations to Oscillatory Dryout Tests

[ ] In some of these experiments, the power was increased beyond the stability threshold and resulted in growing flow rate oscillations. When the flow oscillations were allowed to grow to large magnitudes, some of the thermocouples attached to the inner surface of the electrically heated pins responded with elevated temperature that followed inlet flow minima by a time delay characteristic of the density wave, marking the arrival of the flow minimum to the elevation of the thermocouple. The temperature response is clearly indicative of degraded heat transfer.[††] Cyclic dryout and rewetting have been observed in several tests, where dryout is indicated by sharp temperature increases, followed by temperature decay indicating rewetting.

RAMONA5-FA was used to simulate these cyclic dryout and rewetting tests [ ]

Plots showing the results of the sensitivity study are shown below. These results demonstrate that the CPR correlations perform adequately under transient testing conditions. In summary,

- The time of MCPR [ ] coincides with the time of peak heater surface temperature, indicating the proper density wave propagation time characteristics as modeled by RAMONA5-FA.
- The heater surface temperature response indicating dryout correlates well with MCPR=1 predictions [ ]

[††] [ ]

- [

  ]

- [

  ]

Figure 3-1 Dryout Results for [ ]

Figure 3-2 Dryout Results for [ ]

Figure 3-3 Dryout Results for [ ]

Figure 3-4 Dryout Results for [ ]

Figure 3-5 Dryout Results for [ ]

Figure 3-6 Dryout Results for [ ]

3.3 Local Effects – Radial Power Peaking

The section is devoted to the proper consideration of the effect of radial power peaking, which is mandated by Reference 17.

[

]

[

]

[

] This method is sufficient to cover the required radial power peaking consideration required in the Reference 17 guideline. [

]

‡‡ [

]

3.4 DIVOM Phenomena Ranking Table

A phenomena ranking table, following the BWROG list (Reference 17), has been prepared. The table given below is restricted to the high ranking parameters where some of the medium ranking parameters from Reference 17 have been elevated to high ranking. The phenomena listed below have been dispositioned [

]

Table 3-1 DIVOM Phenomena Ranking Table

Table 3-1 DIVOM Phenomena Ranking Table (continued)

3.5 Applicable Plant Operating Modes

The DIVOM analysis results determined using the plant and cycle-specific methodology defined in this report are applicable for the normal operating and licensing envelope for current BWRs. This includes:

- Normal operating power/flow operating maps. This includes lower flows up to the Maximum Extended Load Line Limit Analysis / Maximum Extended Operating Domain (MELLLA/MEOD) operating boundaries and higher flows up to the Increased Core Flow boundaries.

- Normal Equipment Out-Of-Service (EOOS) options:

    - Single Loop Operation (SLO) is acceptable since the licensing basis is protecting against the regional mode oscillations which are not sensitive to the recirculation system modeling. Furthermore, the SLMCPR for SLO includes adjustments to account for the increased flow uncertainty and LPRM noise inherent in SLO.

    - Recirculation Pump Trip and Turbine Bypass Valve Out-Of-Service (OOS) are EOOS options used to mitigate the delta-CPR response during fast-pressurization events. Therefore, the lack of these systems has no effect on the operation of the OPRM system.

    - Feedwater Heater Out-Of-Service (FHOOS) and Final Feedwater Temperature Reduction (FFTR) involve taking feedwater heaters off-line with a resulting decrease in feedwater temperature and increase in core inlet subcooling. DIVOM is not sensitive to the effects of inlet subcooling as mentioned in Section 3.8 of the BWROG guideline of Reference 17.

4.0 RAMONA5-FA Code Description

The RAMONA5-FA code is the key element of the methodology for DIVOM calculations at FANP. The following sections will detail the evolution of the RAMONA5-FA code version. This will include a brief history of the base RAMONA5 code, and improvements made by FANP.

4.1 The Base RAMONA5 Code

The RAMONA5 code system uses a four equation, non-homogeneous, non-equilibrium, one-dimensional, two-phase flow model. The four equations used describe:

- The liquid mass conservation equation
- The vapor mass conservation equation
- The mixture non-equilibrium energy conservation equation
- The integrated mixture momentum equation with drift flux

The momentum equation is integrated through the vessel flow loop to predict the individual velocities for each vessel component and core channel inlet for each time step. The core model consists of parallel hydraulic channels allowing each individual fuel channel to be modeled separately.

A detailed description of the RAMONA code system can be found in Reference 6. This reference also provides a detailed list of assumptions used in developing the code, and their associated consequences. Also included is a list of recommended code improvements. Several of the important code improvements listed in Reference 6 have already been incorporated into the RAMONA5 Version 2.4 (Reference 18) developed by Studsvik-Scandpower. These improvements include improved modeling of the recirculation pumps through homologous pump curves and the use of parallel downcomer volumes to allow modeling of asymmetric loop operation.

[

]

[

] Detailed descriptions of the changes made to RAMONA5 Version 2.4 are detailed in the next sections.

4.2 Neutron Kinetics Update

[

]

4.2.1 [

]

[

]

4.3 Fuel Pin Model Improvement

[

]

[

]

These improvements allow for a more realistic modeling of the thermal response of a fuel rod based on the local pin conditions.

In addition to the improvements in the fuel rod properties modeling, a more accurate representation of the direct moderator heating was also included. [

] This produces a more accurate model of the heat deposition in the pin.

4.4 Recirculation Loop Improvement

Improvements to the recirculation loop were made to improve the convergence of multiple downcomer volumes when modeling asymmetric (e.g. single loop) operation. These improvements ensure that the multiple loops completely converge during the steady-state calculations. Additional improvements were made to correctly describe the jet pump performance through the use of M/N ratios. These changes together allow for a better characterization and representation of the recirculation system, [

]

4.5 Code Automation

Many of the improvements incorporated in RAMONA5-FA were centered around the automation of input and basic user functions. The purpose of the automation is to improve consistency between RAMONA5-FA and the steady-state code MICROBURN-B2 by automating the transfer of information between the two codes. The automation reduces the time spent by the analyst on gathering data and improves quality by eliminating potential errors in data handling by the analyst. The automation centers around two areas, the automation of input and the automation of features. A discussion of the automation effort is described in the sections below.

4.5.1 Automation of Input

[

]

4.5.2 Automation of Features

[

]

4.6 Closing Relations and Correlations

RAMONA5-FA is designed to perform transient calculations based on steady state initial conditions for the neutronic and thermal-hydraulic models from the MICROBURN-B2 output. It is therefore desirable to achieve the highest possible level of consistency in modeling between the two codes. The base version from Studsvik-Scandpower (RAMONA5-2.4) includes a variety of hydraulic correlation options to suit a variety of user needs. [

]

[

]

The standard FANP methodology in current use for core design includes the correlation set [

] The following sections discuss the correlations included in RAMONA5-FA along with the recommended model set for DIVOM analysis.

4.6.1 Void-Quality Correlation

The original RAMONA5 Version 2.4 contains several options for the void-quality correlations, specifically the correlations of interest are the Bankoff-Malnes and the Chexal-Lellouche correlations. [

]

The Bankoff-Malnes correlation is the Studsvik-Scandpower recommended void-quality correlation. This correlation is dependent on user defined coefficients. [

]

[

]

The Chexal-Lellouche correlation was included in RAMONA5 Version 2.4. [

]

4.6.2 Pressure Drop Correlations

In order to maintain consistency with MICROBURN-B2, [

] The use of these correlations in RAMONA5-FA has been included in the demonstration and benchmarking analyses, which qualifies them for use in the DIVOM analyses.

4.6.3 Nonequilibrium Boiling Correlation

The base version of RAMONA utilizes a mechanistic nonequilibrium phase change correlation with a user-defined set of coefficients. This nonequilibrium boiling model covers the regime of subcooled boiling, which is a rather sensitive parameter for stability calculations. [

]

4.6.4 Dryout Correlations

The DIVOM response is a relative CPR response, and any dryout correlation should be able to calculate this relative change accurately. [ ]

[

]

The ANFB-10 (Reference 19) and SPCB (Reference 20) correlations have been implemented in RAMONA5-FA. These two correlations are the current licensing dryout correlations in the US. They are both qualified and can be used for DIVOM analyses for FANP fuel or other vendor's fuel. [

]

5.0 RAMONA5-FA Code Validation

In order to validate the functions and additions to the RAMONA5-FA code, several sets of benchmarks were performed. [

] utilize neutronic input taken from the benchmark material used to qualify the frequency domain code STAIF (Reference 9).

5.1 [

]

§§ [

]

[

]

5.2 [

]

5.3 [

]

5.4 [

]

5.5 [

]

*** [

]

[

]

[

]

[

]

Figure 5-1 RAMONA5-FA calculated versus measured decay ratio [ ]

Figure 5-2 RAMONA5-FA calculated versus measured frequency [

]

Figure 5-3 RAMONA5-FA calculated versus measured [ ]

6.0 DIVOM Sensitivities

This section presents the results of example DIVOM calculations and discusses the sensitivities of the DIVOM curves to several input parameters.

The core selected for use in this sensitivity study is a typical 764 bundle reactor core. This core is used to provide the nuclear cross sections for both the global and regional modes.

The sensitivity of the DIVOM curve slope to the following parameters has been addressed:

1. [
2.
3.
4.
5.
6.
7.
8.
9.
10.
11.
12.
13.
14.]

The results are plotted in a group of 4 plots per case. These are described below:

1. DIVOM points. The original generic DIVOM line, slope of 0.45, is also shown.

2. Time trace of the global and regional power oscillation signals, [

]

3. Time trace of the power, flow, and critical power ratio for the all-time maximum power swing bundle
4. Time trace of the power, flow, and critical power ratio for the all-time maximum CPR swing bundle

In addition to the 4 plots, a table provides the weighted average DIVOM slope and the maximum DIVOM slope for each case. [

]

The weighted average slope parameter and the maximum slope are used as indicators of the DIVOM sensitivity, because a strictly defined slope is possible only when DIVOM points form a straight line. In the application of the DIVOM points, the curve is defined as a piecewise linear function, i.e. linear interpolation is applicable between two successive points. The overall slope indicators defined here are used to characterize the general sensitivity and are not meant for use directly in the determination of the setpoint for the Detect & Suppress system.

As will be detailed in the next sections, the DIVOM methodology is demonstrated to be robust, in the sense that the sensitivity of DIVOM slope indicators to the variation of input parameters is continuous and relatively small. The results of the sensitivity study are summarized in Table 6-1.

6.1 DIVOM Base Case

The basic data for the base case run are listed below:

[

]

The results of the base case run are given in Figure 6-1. Data differing from the above list will be indicated for each case.

6.2 [

]

6.3 [

]

[

]

6.4 [

]

6.5 [

]

6.6 [

]

6.7 [

]

[

]

6.8 [

]

6.9 [

]

6.10 [

]

6.11 [

]

6.12 [

]

[

]

6.13 [

]

6.14 [

]

6.15 [

]

6.16 [

]

6.17 [

]

6.18 [

]

6.19 [

]

6.20 [

]

6.21 [

]

---

††† [

]

6.22 [

]

6.23 [

]

6.24 [

]

6.25 [

]

6.26 [

]

6.27 [

]

Table 6-1 Sensitivity Study Results

Table 6-2 Sensitivity Study Results (continued)

Average and limiting DIVOM slopes are calculated for the limiting core half only.

Figure 6-1 DIVOM Results for the Regional Mode, Base Case

Figure 6-2 DIVOM Results for the Regional Mode, [ ]

Figure 6-3 DIVOM Results for the Regional Mode, [ ]

Figure 6-4 DIVOM Results for the Regional Mode, [ ]

**Figure 6-5 DIVOM Results for the Regional Mode, [
]**

**Figure 6-6 DIVOM Results for the Regional Mode, [
]**

Figure 6-7 DIVOM Results for the Regional Mode, [ ]

Figure 6-8 DIVOM Results for the Regional Mode, [ ]

**Figure 6-9 DIVOM Results for the Regional Mode, [
]**

**Figure 6-10 DIVOM Results for the Regional Mode, [
]**

Figure 6-11 DIVOM Results for the Regional Mode, [ ]

Figure 6-12 DIVOM Results for the Regional Mode, [ ]

**Figure 6-13 DIVOM Results for the Regional Mode, [
]**

Figure 6-14 DIVOM Results for the Regional Mode, [ ]

**Figure 6-15 DIVOM Results for the Regional Mode, [
]**

Figure 6-16 DIVOM Results for the Regional Mode, [ ]

**Figure 6-17 DIVOM Results for the Regional Mode, [
]**

Figure 6-18 DIVOM Results for the Regional Mode, [ ]

Figure 6-19 DIVOM Results for the Regional Mode, [ ]

Figure 6-20 DIVOM Results for the Regional Mode, [ ]

Figure 6-21 DIVOM Results for the Regional Mode, [ ]

Figure 6-22 DIVOM Results for the Regional Mode, [ ]

Figure 6-23 DIVOM Results for the Regional Mode, [ ]

Figure 6-24 DIVOM Results for the [ ]

Figure 6-25 DIVOM Results for the [ ]

Figure 6-26 DIVOM Results for the [ ]

Figure 6-27 DIVOM Results for the [ ]

Figure 6-28 DIVOM Results for the [ ]

7.0 DIVOM Methodology Application Procedure

The cycle-specific DIVOM analysis entails the analysis of simulated regional oscillations at several state points throughout that cycle. This section is devoted to the general description of the methodology and procedure for performing this calculation. First, the codes, input, and state points for running each simulated regional mode oscillation are described. Second, the DIVOM points and the algorithm used for extracting them by post-processing a simulated regional oscillation are described.

The procedure outlined in this section is consistent with the general BWROG guideline (Reference 17). In summary, the application procedure includes the following elements:

1. [

2.

3.

4.

5.

6.

7.

]

A reduced scope of parameter variations can be considered on a case-by-case basis for subsequent reload analysis. The basis for any reduced scope should be justified and

documented per Section 4.1 of the BWROG guideline of Reference 17. [

]

7.1 Definition of DIVOM Points

The algorithm for calculating DIVOM points follows closely the description given in Reference 17, generalized to include all bundles in the core simultaneously. The main elements in the DIVOM algorithm are given below.

[

]

[

]

8.0 References

1. "BWR Owners' Group Long Term Stability Solutions Licensing Methodology," -- Licensing Topical Report," GE Nuclear Energy, NEDO-31960 (May 1991).

2. C. R. Lehmann (PP&L), M. P. LeFrancois (Yankee Atomic), W. R. Mertz (Southern Nuclear), Hung Le (GE), and Jason Post (GE), "Reactor Stability Detect and Suppress Solutions Licensing Basis Methodology for Reload Applications --- Licensing Topical Report," GE Nuclear Energy, NEDO-32465-A (August 1996).

3. Letter, J.S. Post (GE) to Document Control Desk United States Nuclear Regulatory Commission, "Stability Reload Licensing Calculations Using Generic DIVOM Curve," August 31, 2001.

4. Letter, Jason S. Post (GE) to Document Control Desk United States Nuclear Regulatory Commission, "Stability Reload Licensing Calculations Using Generic DIVOM Curve," June 29, 2001.

5. Presentation to USNRC by Mike May (Exelon Corp.), "Stability Option III DIVOM Part 21 Closure Plan," August 15, 2003.

6. W. Wulff, H. S. Cheng, D. J. Diamond, and M. Khatib-Rahbar, "A Description and Assessment of RAMONA-3B MOD.0 CYCLE 4: A Computer Code with Three-Dimensional Neutron Kinetics for BWR System Transients," NUREG/CR-3664, 1984.

7. Y. M. Farawila and D. W. Pruitt, "Application of Modal Neutron Kinetics to Boiling Water Reactor Oscillation Problems," Nuclear Science and Engineering: 129, 261-272 (1998).

8. XN-NF-84-105(P)(A) Volume 1 and Volume 1 Supplements 1 and 2, *XCOBRA-T: A Computer Code for BWR Transient Thermal-Hydraulic Core* Analysis, Exxon Nuclear Company, February 1987.

9. EMF-CC-074(P)(A) Volume 4 Revision 0, *BWR Stability Analysis – Assessment of STAIF with Input from MICROBURN*-B2, Siemens Power Corporation, August 2000.

10. T. H. J. J. van der Hagen, "The influence of direct energy deposition on BWR stability," Annals of Nuclear Energy 28 (2001) 1447-1456

11. Y. M. Farawila and D. W. Pruitt, "Critical Power Response to Power Oscillations in Boiling Water Reactors," Nuclear Science and Engineering: 143, 211-225 (2003).

12. J. March-Leuba and E. D. Blakeman, "A Mechanism for Out-of-Phase Power Instabilities in Boiling Water Reactors," Nuclear Science and Engineering: 107, 173-179 (1991).

13. R. Miró et al., "On the Regional Oscillation Phenomenon in BWR's," Progress in Nuclear Energy, Vol. 36, No. 2, pp. 189-229, 2000.

14. Y. M. Farawila and D. W. Pruitt, "A Study of Preferred BWR Oscillation Mode Using the STAIF Code," Trans. Am. Nucl. Soc. 71, 441-442 (Nov. 1994).

15. J. March-Leuba, "Density-Wave Instabilities in Boiling Water Reactors," NUREG/CR-6003, ORNL/TM-12130, Sept. 1992.

16. A. Dokhane, "BWR Stability and Bifurcation Analysis using a Novel Reduced Order Model and the System Code RAMONA," Ph.D. Thesis, École Polytechnique Fédérale de Lausanne - Switzerland, 2004.

17. GE-NE-0000-0028-9714-R0, "Plant-Specific Regional Mode DIVOM Procedure Guideline," June 14, 2004.

18. RAMONA5 Version 2.4, "Users and Theory Manuals," Studsvik-Scandpower.

19. EMF-1997(P)(A) Revision 0, *ANFB-10 Critical Power Correlation*, Siemens Power Corporation, July 1998.

20. EMF-2209(P)(A) Revision 2, *SPCB Critical Power Correlation*, Framatome ANP, Inc., September 2003.

21. EMF-2245(P)(A) Revision 0, *Application of Siemens Power Corporation's Critical Power Correlations to Co-Resident Fuel,* Siemens Power Corporation, August 2000.

Distribution

Email Notification

Erlangen

Stefan Opel
Franz Wehle
Florin Curca-Tivig

Richland

BWR Neutronics
BWR Safety Analysis
Codes and Methods